Chapter – 5

Measurement of $^{183}W(n, p)^{183}Ta$ and $^{184}W(n, p)^{184}Ta$ reaction cross section in ^{252}Cf neutron field

---

Publication related to this chapter:

Rajnikant Makwana, S. Mukherjee, L. Snoj, S. S. Barala, M. Mehta, P. Mishra, S. Tiwari, M. Abhangi, S. Khirwadkar, H. Naik, "Measurement of $^{183}W(n, p)^{183}Ta$ and $^{184}W(n, p)^{184}Ta$ reaction cross section"

Applied Radiation Isotopes,

http://dx.doi.org/10.1016/j.apradiso.2017.06.002

Impact Factor 1.136

5.1 Introduction

In the recent decades, there is an overwhelming demand of nuclear reaction cross section data compilation for the development of reactor science and technology. In the International Thermonuclear Experimental Reactor (ITER), fusion reaction process can be studied using the DT reaction. It produces neutrons with an energy of 14.1 MeV, and these neutrons are transmitted through the first wall of the reactor material [1 - 6]. First wall, divertor, blanket, and shielding are the main parts of the fusion reactor. The first wall, divertor and blanket are directly exposed to the DT plasma and bear the maximum amount of the neutron flux (~10^{15} n/cm^2/s). Divertor collects and exhausts heat and particles (neutral and charge), and the reactor walls scatter these neutrons from 14.1 MeV to the thermal neutron energy. Tungsten has been selected as divertor material for ITER [7]. It will face all the neutrons with energies from thermal to 14.1 MeV. These neutrons can open various reaction channels such as (n, γ), (n, p), (n, 2n), (n, d), (n, α) etc. in the reactor materials. It demands complete nuclear reaction cross section data for the different isotopes of tungsten i.e., ^{183,184}W, as they can produce different radioisotopes in the reactor [8]. It is very important as a part of reactor maintenance using remote handling. The reactions ^{183}W(n, p)^{183}Ta and ^{184}W(n, p)^{184}Ta are considered here for the cross section measurement using the ^{252}Cf spontaneous neutron source. There are plenty of experimental data available at 14 MeV for these reactions; however, very few measured data are available for energy range from thermal to 14 MeV. Cross sections at low MeV energy are relatively very important as there are very few measurements and considering the small value of (n, p) reaction cross section. The objective of the present work is to have accurate measurements of the cross section of the above mentioned reactions. Further, the measured data are important to validate evaluated data libraries for tungsten isotopes from different national projects (e.g., ENDF-B/VII.1[9], JENDL-4[10], FENDL[11], ROSFOND [12], CENDL-3.1 [13], JEEF-3.2 [14] etc. In the present chapter, measurement of the cross sections for such nuclear reactions have been discussed.

5.2 Experimental Details

5.2.1 Neutron Source and Target

The $^{252}Cf(sf)$ neutron field is a reference neutron spectra which is considered to be very well known. Mannhart evaluation [15-16] is currently accepted to be the best representation of this reference neutron spectra. Numerical data for this evaluated spectra are available from the IAEA IRDFF web page of IAEA [17]. The average neutron energy in the ^{252}Cf spectrum is 2.124 MeV. The ^{252}Cf isotope is an intense neutron emitter that decays by alpha emission (~ 96.31%) and spontaneous fission (~ 3.09%) with a half-life of 2.645 y. Its neutron emission rate is 2.314×10^6 n/s/μg [18].

A ^{252}Cf neutron source irradiation facility is available at the Defense Laboratory Jodhpur (India). This source is shielded with paraffin, borated wax and lead as shown in FIG 5.1(a). The irradiation of tungsten (W) sample was done by using this portable ^{252}Cf neutron source, having present neutron yield of 1.6064×10^8 n/s. Standard neutron activation analysis technique was used in the present measurements. In this method, a sample with proper weight is required to irradiate with neutrons. It is necessary to produce the desired isotope from this irradiation for the measurement of the selected nuclear reaction cross section. The tungsten sample with purity of 99.97 % was chosen for irradiation. The sample chosen for the irradiation was having dimensions of 8 mm × 8 mm × 5 mm and weighs 6.033 gm.

5.2.2 Neutron Irradiation

The sample was kept at a distance of 60 mm from the ^{252}Cf neutron source for 603 hours for continuous long irradiation. The average neutron spectrum inside the sample was calculated using the Monte Carlo N-Particle Code (MCNP), which is discussed in the next section. After irradiation, the sample was brought to the Neutronics Laboratory, Institute for Plasma Research (IPR), Gandhinagar, India, for counting purpose. The activated sample was kept near the window of the HPGe detector. An HPGe detector with 16K MCA manufactured by CANBERA was used for gamma counting. The counting setup is shown in FIG 5.1 (b). Counting has been done in two different phases; in the first phase a short counting time has been selected, immediately after the irradiation, then after two days of cooling another set of counting was done with larger time. The time of counting was sufficiently long, as the product isotopes have half-life from few hours to few days. The selected nuclear reactions with their necessary details are given in Table 5.1. The gamma spectra obtained from the irradiated sample are shown in FIG 5.2. The cross sections for $^{183}W(n, p)^{183}Ta$ and $^{184}W(n, p)^{184}Ta$ reactions were estimated.

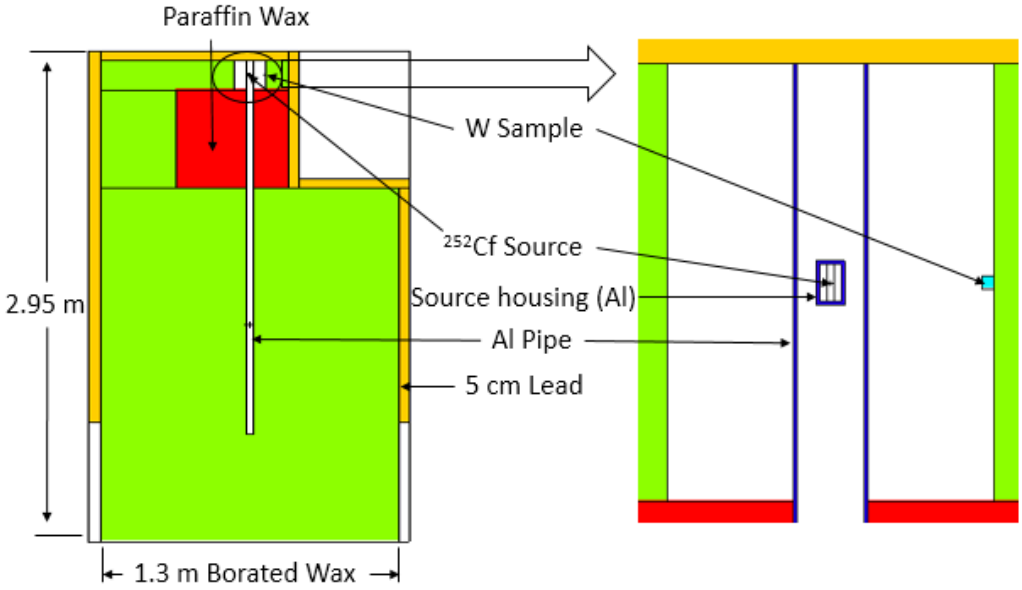

FIG 5.1 (a) MCNP modeling of the irradiation experimental setup

FIG 5.1 (b) Gamma counting setup at IPR, Gandhinagar

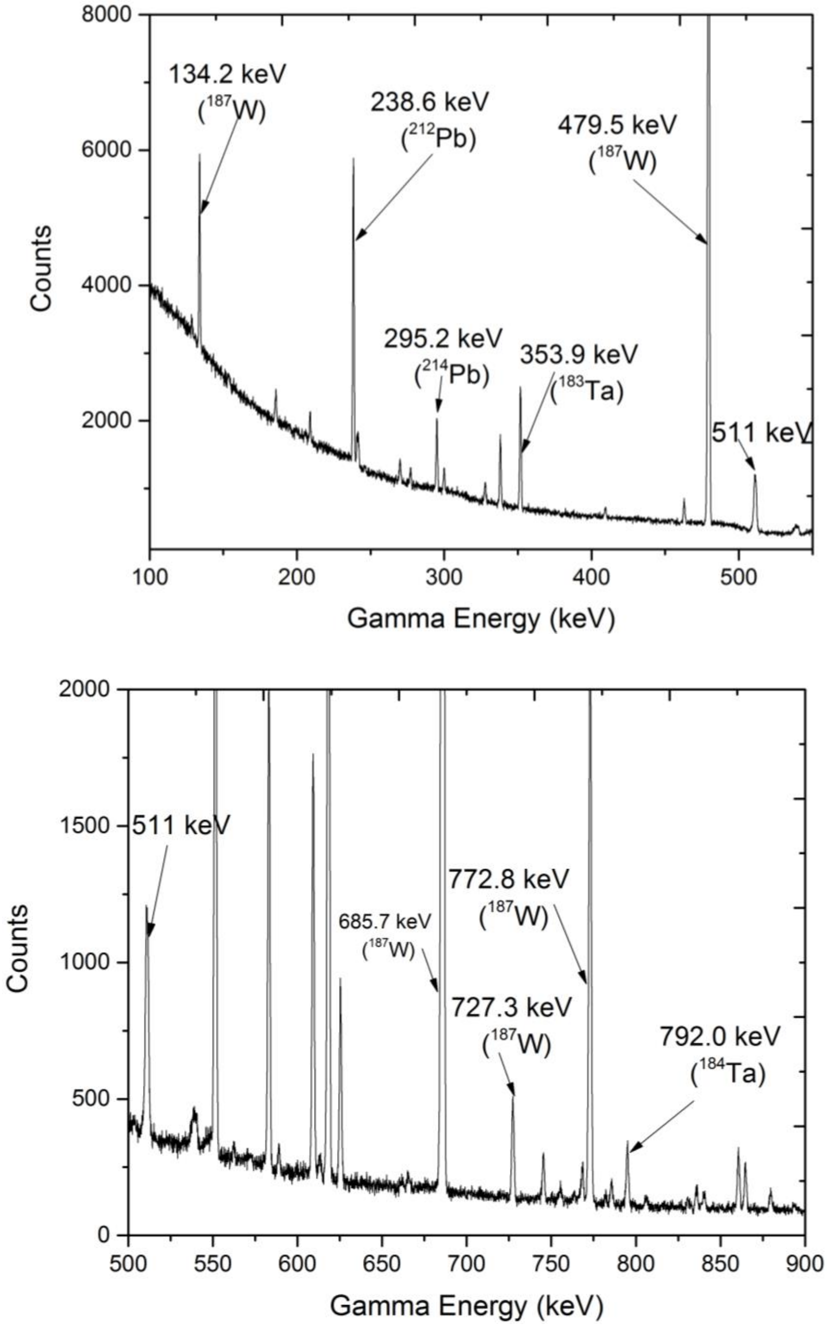

FIG 5.2 Gamma spectrum measured using HPGe detector

Table 5.1 Selected nuclear reactions with isotopic abundance, threshold energy, product half-life, and product gamma energy with its abundance

Reaction	Abundance of Target Isotope (%) [19]	Threshold Energy (MeV) [20]	Half life of product isotope [21]	γ - Energy (KeV)	Γ– Abundance
$^{186}W(n, \gamma)^{187}W$	28.43	-	23.72 h	479.5	21.8
				685.7	27.3
$^{183}W(n, p)^{183}Ta$	14.31	0.29	5.1 d	353.9	11.2
$^{184}W(n, p)^{184}Ta$	30.64	2.095	8.7 h	792.0	14.2

5.3 Theoretical Calculations Using MCNP

This section is divided into two parts; first part discusses the average neutron spectra calculation in the irradiated sample, and on the other hand is related to detector efficiency calculation in the second part. The MCNP – 6.1 code was used to perform these calculations. We have taken help of our collaborator L. Snoj from the Jožef Stefan Institute, Ljubljana, Slovenia for the MCNP calculations. This code has been widely used for the transport of neutron, photon, electron and many other particles. All calculations were performed with ENDF/B-VI cross section data library which comes along with MCNP package. Further, calculations were checked with ENDF/B-VII, in order to find the difference in results, but no significant change was observed in results. The detail of this code has been discussed in earlier Chapter – 2.

5.3.1 Neutron Spectra Calculation

The code MCNP is worldwide used for neutron transport calculation. It is possible to model the actual experimental geometry, with neutron source and material specifications etc. using the code. Once the experimental geometry is modeled, as described in Chapter – 2, the tally card can be used to calculate the neutron spectra at the desired location. It is necessary to model the neutron source accurately for the simulations. The ^{252}Cf source is having continuous neutron spectrum, therefore it was necessary to calculate the averaged neutron spectrum inside the sample. The ^{252}Cf

was modeled using the MCNP code, as explained by L. Snoj *et al*., [22]. The most rigorous approach as explained by L. Snoj *et al*., is to use evaluated neutron spectrum of Mannhart (IRDF-2002 [15-17, 22-23]). In the present work, the average neutron spectra over sample volume have been calculated by using the IRDF – 2002 ^{252}Cf spontaneous fission neutron spectra. Monte Carlo based MCNP code (MCNP – 6.1) with ENDF/B-VII data library was used to model the irradiation assembly as shown in FIG 5.1 (a). The tally F4, which gives volume averaged flux tally was used for the calculation. The definition of the F4 tally is represented by the following relation.

$$F4 = \frac{1}{V}\int_V dV \int_E dE \int_{4\pi} d\Omega\phi(r, E, \Omega) \tag{5.1}$$

where, V = volume of the sample,

E = energy of the neutron

Ω = solid angle

r = radial distance from source

ϕ = flux at distance

The calculated spectrum is shown in FIG 5.3. There has been a significant increment in lower energy neutrons due to scattering from the source shielding. However, the higher energy tail shape remained same as in the pure source spectra.

As the chosen reactions have different threshold energies, entire neutron spectrum was not used to produce the product isotopes. Only those neutrons that were above the threshold energy for both reactions are able to produce the product isotopes. Hence the low energy neutrons below the threshold can be removed from the neutron spectra for both the reactions. This gives the effective neutron spectrum for the respective reaction. This is shown in FIG 5.3(a-c). It can be seen from FIG 5.3(a), that the whole neutron spectrum contains a very large contribution from low energy (thermalized) neutrons, which are backscattered from the surrounding shielding materials. As our chosen reactions have a threshold above these neutron energies, they do not interfere. The effective neutrons spectra are shown for both reactions in FIG 5.3(b-c). Again there is a very small number of neutrons available above 4.5 MeV neutrons. The ratio of these neutrons to total neutrons is < 6 %. So the major contribution in the reaction product is due to the neutrons from threshold to 4.5 MeV neutrons. Therefore, the measure cross section can be reported at the spectrum averaged energy for these neutrons. Following formula has been used to calculate the spectrum averaged energy from the calculated neutron spectra in the irradiated sample, which is known as the effective mean energy/spectrum [24],

$$E_{mean} = \frac{\int_{E_{th}}^{E_{max}} E_i \phi_i dE}{\int_{E_{th}}^{E_{max}} \phi_i dE} \quad 5.2$$

where,

E_{th} = threshold energy of the reaction

E_{max} = maximum neutron energy

E_i = energy bin

ϕ_i = neutron flux in energy bin E_i

E_{mean} = effective mean energy

This mean energy is used to quote for the measured cross section values.

5.3.2 Detector Efficiency Calibration

The HPGe detector, which was used for the activation measurement having crystal size of 64.80 mm diameter and 64.60 mm length. The window thickness is 0.60 mm and made of carbon composite. The efficiency of the detector was measured for the different gamma ray energies using mix-energy gamma source available at IPR, Gandhinagar, India. A mix-energy gamma source is contains different radioactive isotopes, such as ^{241}Am (59.54 keV, 919.19 Bq), ^{109}Cd (88.03 keV, 4.132 kBq), ^{57}Co (122.06, 136.47 keV, 144.85 Bq), ^{139}Ce (165.85 keV, 5.050 kBq), ^{51}Cr (320.08 keV, 0.09 Bq), ^{113}Sn(391.69 keV, 91.06 Bq), ^{85}Sr (514.00 keV, 11.85 Bq), ^{137}Cs (661.65 keV, 1.712 kBq), ^{88}Y (898.03 keV, 152.45 Bq), ^{60}Co (1173.22, 1332.49 keV, 2.183 kBq) and ^{88}Y (1836.05 keV, 152.45 Bq), that covers gamma energy from 59 keV to 1.8 MeV. Full efficiency curve was plotted using measured photopeak efficiency. In the present measurements, a point source was used to measure detector efficiency. However, in the actual experiment, the volume sample was used. Therefore, it was necessary to obtain efficiency for the volume source of the sample dimension. Further, the volume source attenuates photons from the subsequent layers towards the detector, and, a large number of photons are scattered from the backside layers of the sample. To study the self-shielding and back scattering effect from the W sample, another measurement has been carried out. The method used has been described in reference [25]. The W samples with the thickness of 1, 2, 3 and 5 mm were kept in between source and detector. In this arrangement, the gammas emitted from the source were attenuated by the sample. The results are shown in FIG 5.4. It is clear from this figure, that the efficiency will be different for the volume source, due to attenuation. Also, the backscattering has a significant contribution.

The efficiency of the volume sample by considering backscattering and self-shielding effect can be calculated using the MCNP code. In this context, the detector was modeled by using this code as shown in FIG 5.5. The experimentally measured efficiency at various distances using the point gamma source, at different energies were calculated and compared with simulated efficiency in FIG 5.6(a). The model was optimized by getting the ratio of calculated efficiency to experimental efficiency (C/E ratio) ~ 1, which is shown in FIG 5.6(b). This model was used for the actual sample – detector geometry to estimate the efficiency of the detector. This method considers both the self-shielding and back scattering effect due to the volume of the sample. This efficiency values for different selected gamma energies were used to calculate the cross section using neutron activation technique.

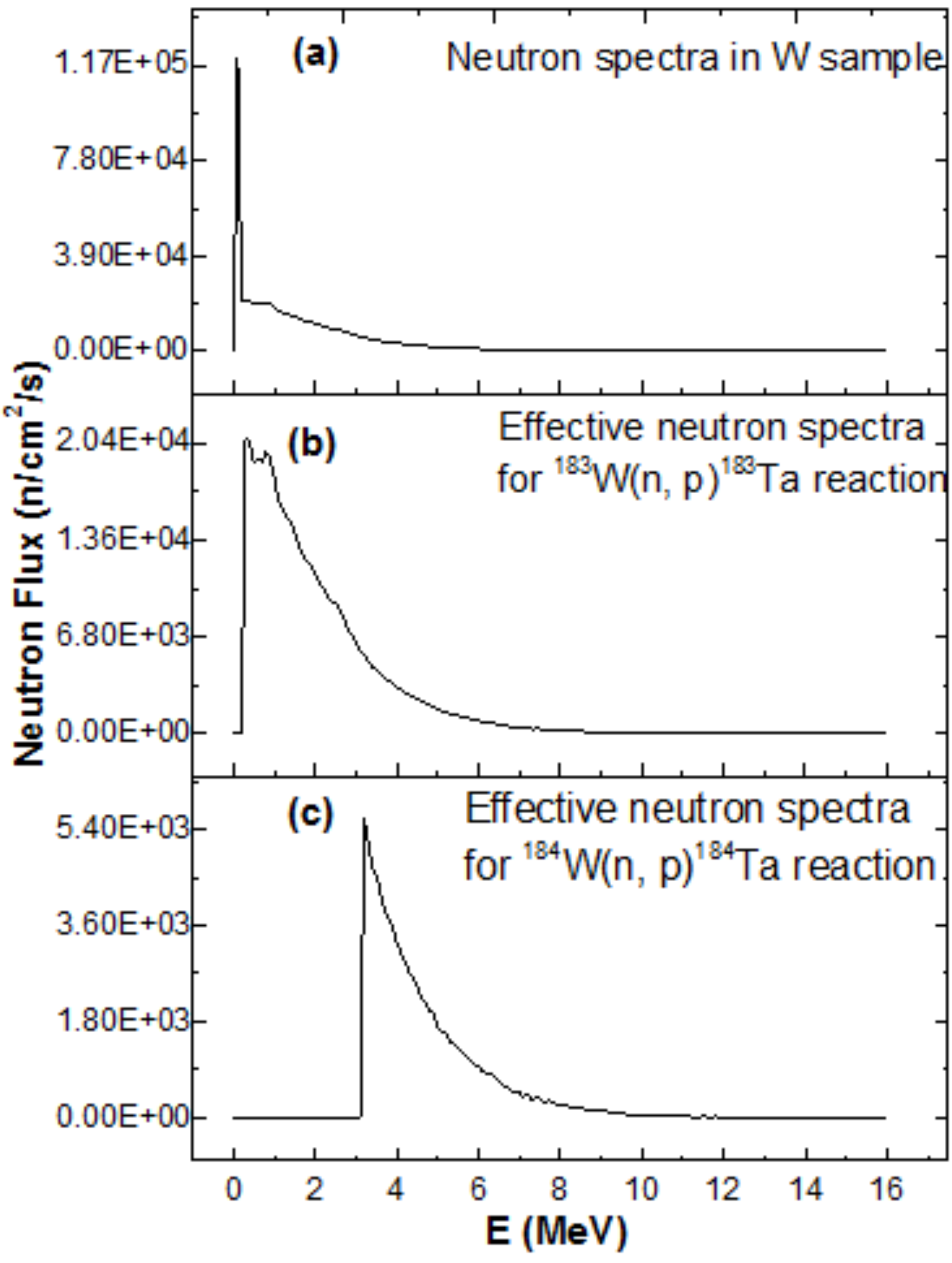

FIG 5.3 ^{252}Cf Source neutron spectra – average neutron spectra in W sample, and the effective neutrons for the selected reactions, which are above the threshold energy of the reactions

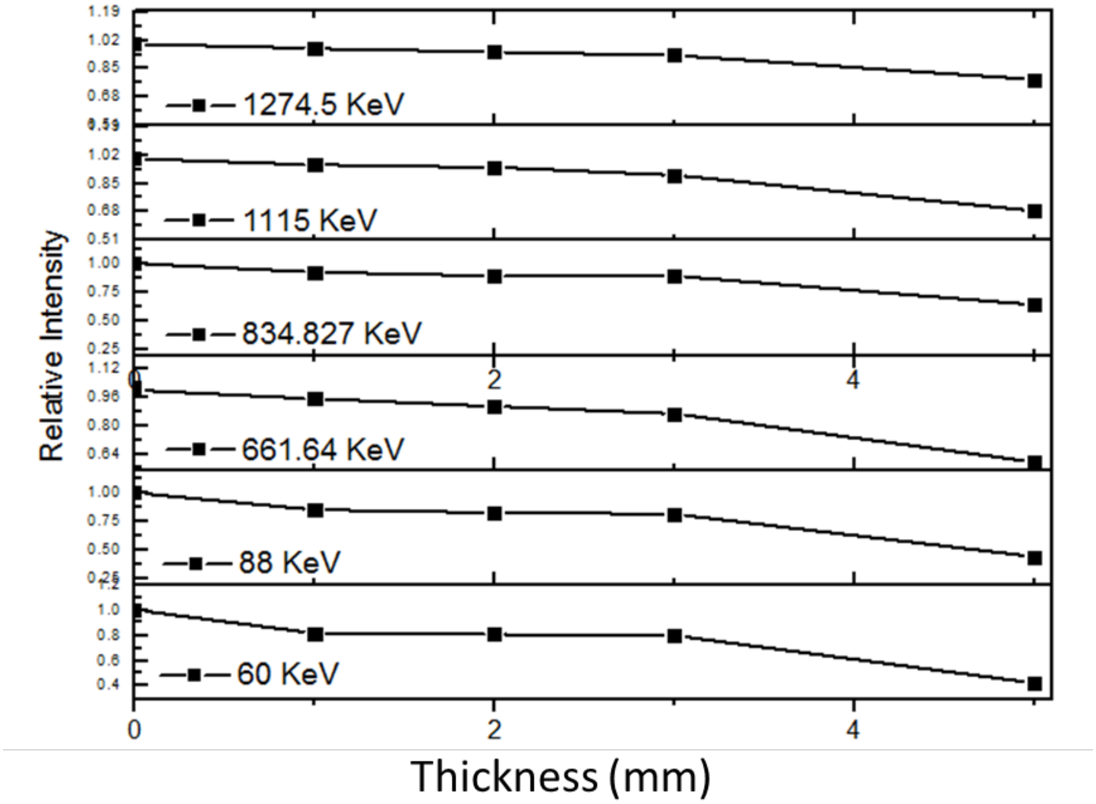

FIG 5.4 Relative intensity showing the self-shielding effect increases as the thickness of the sample increases

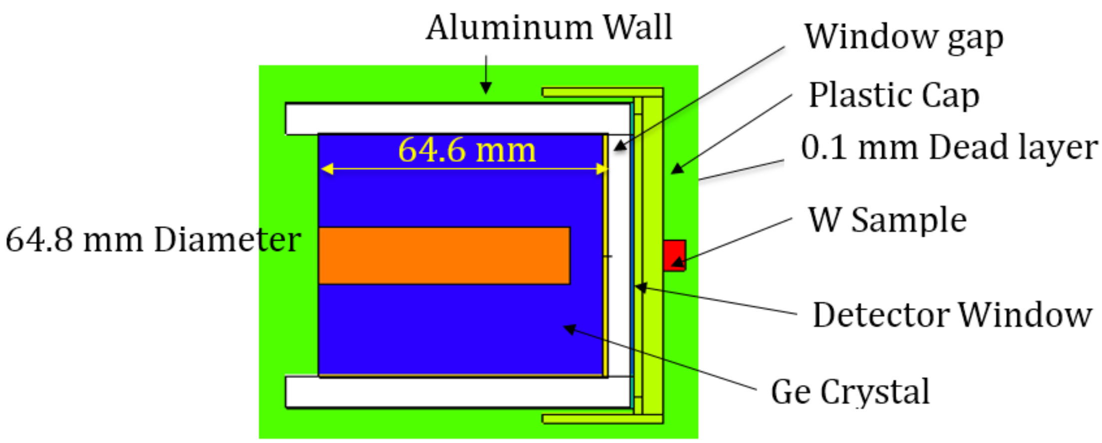

FIG 5.5 MCNP Model of the detector to calculate efficiency for irradiated volume sample placed on end cap of the detector

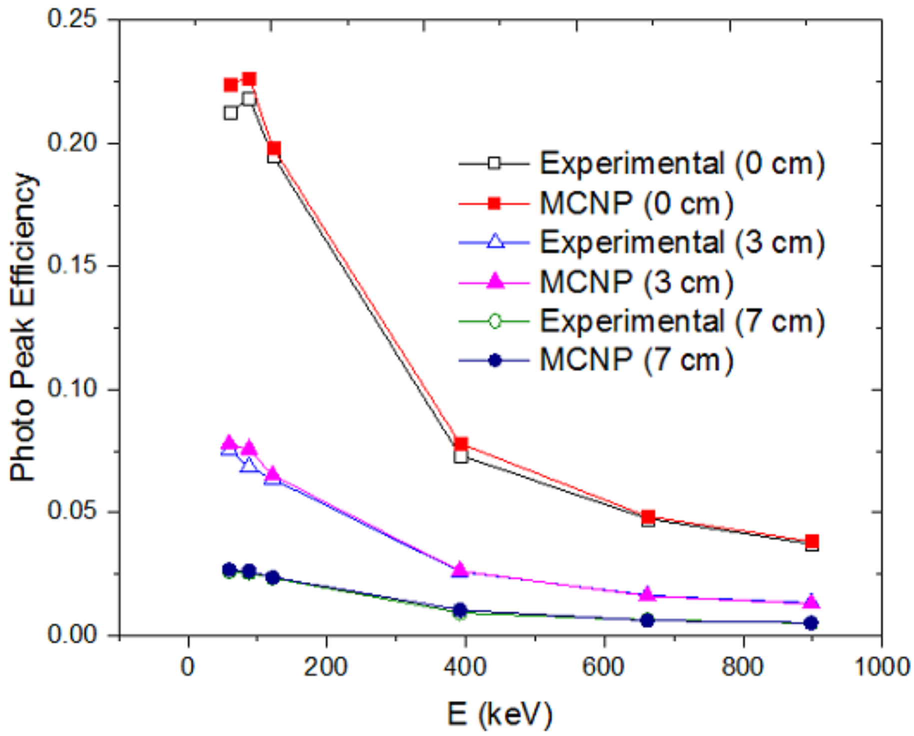

FIG 5.6(a) Comparison of measured and MCNP calculated detector efficiency at various gamma energies

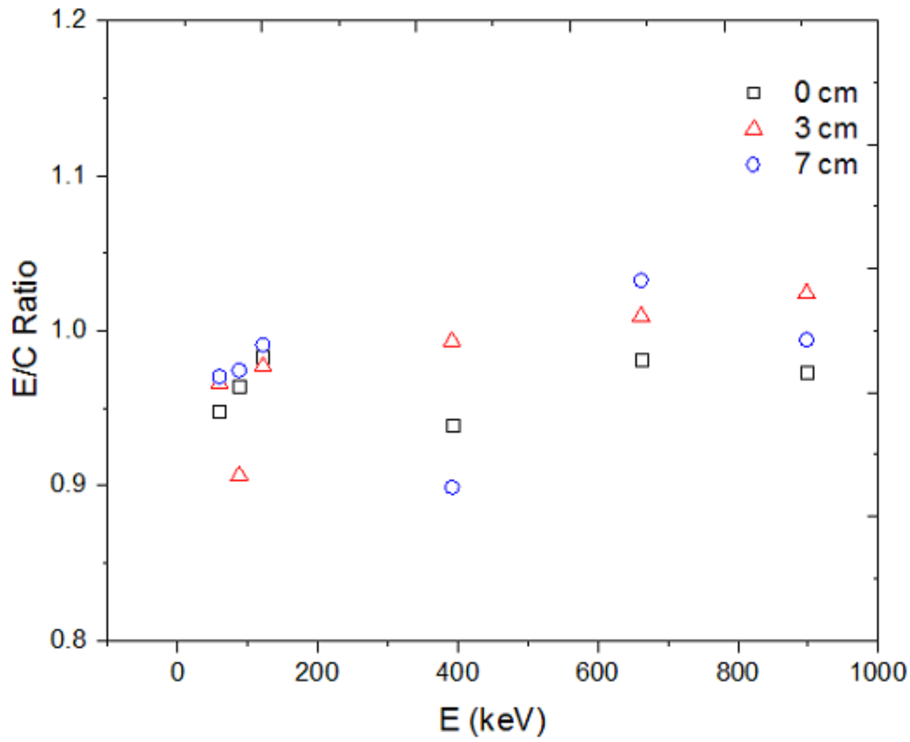

FIG 5.6(b) Comparison of Experimental to MCNP calculated detector efficiency ratio at various gamma energies

5.4 Data Analysis – Neutron Activation Analysis

The neutron activation analysis has been already discussed in Chapter – 4. The measured data along with the calculated efficiency and neutron flux using MCNP were used to calculate the reaction cross sections. The production cross section (σ) of the interested isotope from the desired reaction was obtained by using the following standard activation equation,

$$\sigma = \frac{A_I \cdot A_\gamma \cdot \lambda}{(\emptyset \theta_\gamma \epsilon_\gamma w_i P_i N_{av}) \cdot (1-e^{-\lambda t_i}) \cdot (1-e^{-\lambda t_c}) \cdot e^{-\lambda t_w}} \qquad 5.5$$

Where, A_I = Gram Atomic Weight of the target

A_γ= Peak Counts of gamma energy

λ = Decay constant of product nucleus (s^{-1})

t_i = irradiation time

t_w = Cooling time

t_c = Counting time

$\emptyset$ = Incident neutron flux

θ_γ = γ intensity

ϵ_γ = Efficiency of detector at gamma chosen

w_i = weight of sample (gm)

P_i = Abundance of target isotope

N_{av} = Avogadro's number

The photopeak counts of the gamma rays emitted from the desired isotope were carefully measured from the gamma spectrum. The selected gamma energies along with their abundances for the desired radioisotopes are given in Table 5.1. The measured cross sections for the selected reactions are given in Table 5.2.

5.5 Nuclear Modular Code Prediction

In order to support the present measured nuclear cross section data, nuclear modular calculations were performed by using EMPIRE – 3.2.2 code. This code uses different nuclear models to predict nuclear reaction cross section. It can predict nuclear reaction data for neutron, gamma, proton, deuteron, triton, ^{3}He and alpha with an energy range from few keV to several hundreds of MeV. The EMPIRE – 3.2.2 uses reaction parameters from Reference Input Parameter Library (RIPL) – 3. It considers the effect of level density, and all three nuclear reaction mechanisms: compound, pre-equilibrium, and direct reaction. The optical model parameters were obtained by using a global potential proposed by Koning and Delaroche [26]. The compound reaction mechanism was incorporated by Hauser-Feshbach model [27]. The pre-equilibrium contribution was included by exciton model, developed by Kalbach [28]. The details of these codes have been discussed in Chapter – 2.

In the present case, different parameters such as level density parameters were used to evaluate the cross section of the interested nuclear reactions. The calculated reaction cross sections for the production of selected radioisotopes were used to compare the measured reaction cross sections shown FIGS 5.7 – 5.8.

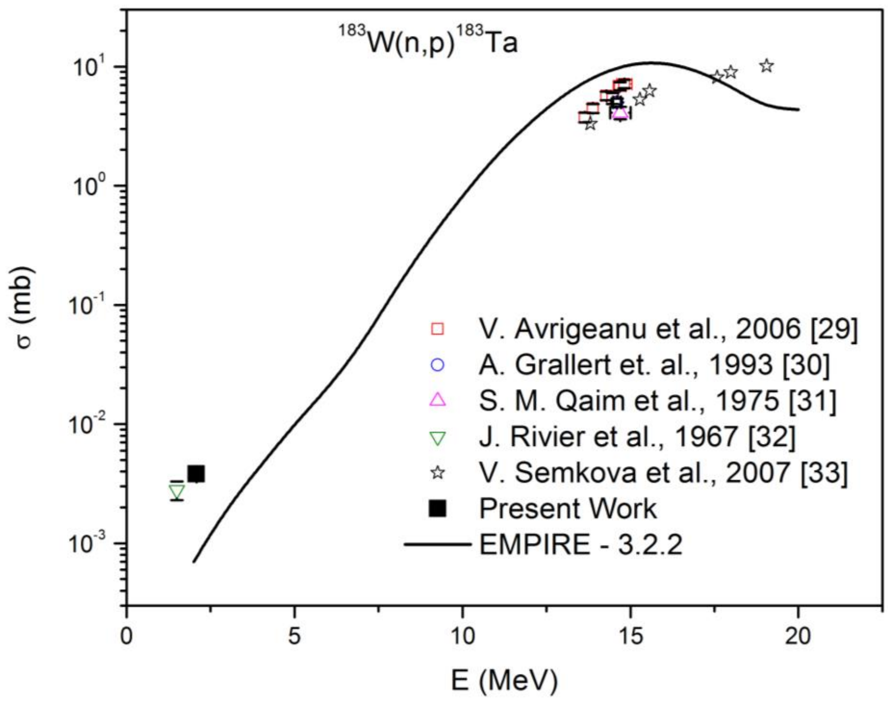

FIG 5.7 Comparison of present measured spectrum averaged cross section with experimental and EMPIRE-3.2.2 evaluated cross section for $^{183}W(n, p)^{183}Ta$; the present data and data point of J. Rivier et al., [32] are spectrum averaged cross sections, other experimental data are for mono energy neutrons

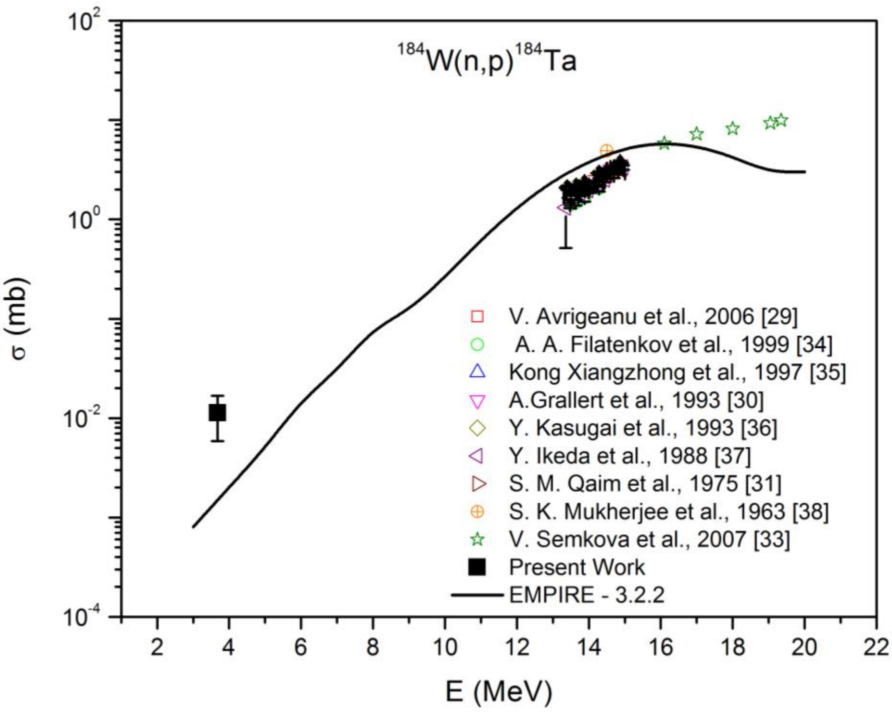

FIG 5.8 Comparison of measured cross section with experimental and EMPIRE-3.2.2 evaluated cross section for $^{184}W(n, p)^{184}W$

5.6 Results and discussion

The cross sections were measured with improved accuracy, with the application of simulation technique, which incorporates, self-shielding, backscattering, volume source effect in efficiency etc. Geometrical effect and shielding effect on average neutron spectra inside the sample were calculated using MCNP simulation. To the best of our knowledge, the present measurements have been done for the first time in the above mentioned neutron energies. The effect of self-attenuation and backscattering, and the sample-volume geometry effect on the efficiency of the detector was corrected by optimizing MCNP model of the HPGe detector at different distances and for different energies of a gamma photon. The parameters for the error propagation in the final cross section estimations were considered. Major error contributions in the present data are due to relative efficiency (2 – 3 %), scattered neutron (1 – 3 %), statistical error (3 – 4 %), detector dead time (< 2 %). The overall error in the present measurement was < 6 %.

The EMPIRE – 3.2.2 nuclear modular code was used for evaluating the cross section of the selected nuclear reactions. The measured data were compared with the evaluated data and available data in EXFOR data library in the FIGS. 5.7 – 5.8 [29 – 38]. In the case of $^{183}W(n, p)^{183}Ta$, there is a previous measurement for this reaction near to the present listed energy, by J. Rivier *et al.*, [32], which is in agreement with the present data. In both the (n, p) reactions the measured cross sections are higher by a small factor in comparison with the evaluated data.

Table 5.2 Measured Cross section for the selected nuclear reactions

Reaction	**Spectrum Average Energy (MeV)**	**Measured Cross section ($\times 10^{-3}$mb)**
$^{183}W(n, p)^{183}Ta$	1.70 ± 1.35	3.8 ± 0.3
$^{184}W(n, p)^{184}Ta$	3.75 ± 1.26	11.3± 0.9

5.7 Summary and Conclusion

In the present measurements, cross sections of $^{183}W(n, p)^{183}Ta$, and $^{184}W(n, p)^{184}Ta$ reactions were measured using a ^{252}Cf neutron source at spectrum averaged energies above the threshold of the reaction to the maximum neutron energy. This is a material of interest for a fusion reactor. The averaged neutron spectra inside the sample volume were calculated using MCNP code. The data that have been presented for (n, p) reactions for the available energies has very few or no previous measurements. The theoretical estimation of the cross section was done by EMPIRE – 3.2.2 code. It may be observed that present experimental results are in agreement within the limits of the experimental error. The study shows that the cross section of (n, p) reaction for tungsten isotopes are having small values. But for the case of the fusion reactor, where the first wall is facing ~10^{15} neutrons/sec/cm^2, it can produce a considerable amount of radioactive waste.

References

[1] J. Qing, Y. Wu, M. Regis, and J. W. Kwan, IEEE Trans. Nucl. Sci., 56 (2009) 1312–1315.

[2] J. Reijonen, et al., Appl. Radiat. Isotopes, 63 (2005) 757–763.

[3] Y. Wu, et al., IEEE Trans. Nucl. Sci., 56 (2009) 1306–1311.

[4] V. Voitsenya et al., Rev. Sci. Instrum., 72 (2001) 475–482.

[5] G. De Temmerman, et al., J. Nucl. Mater., 363 (2007) 259–263.

[6] K. H. Behringer, J. Nucl. Mater., 145 (1987) 145–153.

[7] M. Lehnen, et al., Journal of Nuclear Materials 463 (2013) 39-48.

[8] R. A. Forrest, Energy Procedia 7 (2011) 540–552.

[9] M.B. Chadwick, et al., "ENDF/B-VII.1: Nuclear Data for Science and Technology: Cross Sections, Covariances, Fission Product Yields and Decay Data", Nucl. Data Sheets 112(2011)2887.

[10] Keiichi Shibata, et al., J. Nucl. Sci. Technol.. 48(1), 1-30 (2011).

[11] FENDL-3.1 data library, https://www-nds.iaea.org/fendl31/

[12] ROSFOND data library, http://www.ippe.ru/podr/abbn/english/libr/rosfond.php

[13] Z. G. Ge, et al., Journal of the Korean Physical Society, Vol. 59, No. 2, August 2011, pp. 1052

[14] JEFF-3.2 data library, https://www.oecd-nea.org/dbforms/data/eva/evatapes/jeff_32/

[15] W. Mannhart, IAEA-TECDOC-410 (1987) 158

[16] W. Mannhart, INDC(NDC)-220/L (1989) 305

[17] IRDF-2002, https://www-nds.iaea.org/IRDFF/IRDFF-v1-05_sp.endf

[18] Manojlovič S, et al., Applied Radiation and Isotopes, 101 (2015) 101–106.

[19] K. J. R. Rosman, P. D. P. Taylor, Pure Appl. Chem., 71 (1999) 1593-1607.

[20] Q value calculator, retrieved from: http://www.nndc.bnl.gov/qcalc/index.jsp.

[21] Table of Isotopes decay data, retrieved from: http://nucleardata.nuclear.lu.se/toi/listnuc.asp?Z=74.

[22] Narayan, Pradeep et al., Indian Journal of Pure & Applied Physics, 48 (2010) 798-801.

[23] IAEA, International reactor dosimetry file 2002 (IRDF-2002) Technical Report Series, International Atomic Energy Agency, Vienna (2006) 162.

[24] D. L. Smith, et al., " Corrections for Low Energy Neutrons by Spectral Indexing", Retrieved from: https://www.oecd-nea.org/science/docs/2005/nsc-wpec-doc2005-357.pdf

[25] J. Rama Rao, et al., Nucl. Instrum. Methods Phys. Res., Sect. B, 17 (1986) 368 - 371.

[26] A. J. Koning, and J. P. Declaroche, Nucl. Phys. A713 (2003) 231.

[27] W. Hauser, and H. Feshbach, Phys. Rev. C 87 (1952) 366.

[28] C. Kalbach, Phys. Rev. C 33 (1986) 818.

[29] V. Avrigeanu, et al., Nucl. Phys. A 765 (2006) 1.

[30] A. Grallert, et al., Rept.: IAEA Nucl. Data Section report to I.N.D.C. No. 286 (1993) 131.

[31] S. M. Qaim, and C. Graca, Nucl. Phys. A 242-2 (1975) 317.

[32] J. Rivier, et al., Jour. Radio Chemica Acta. 8 (1967) 1967.

[33] V. Semkova, R. Capote, R. Jaime Tornin, A. J. Koning, A. Moens, and A. J. M. Plompen, DOI: 10.1051/ndata:07320.

[34] P. Reimer, V. Avrigeanu, S. V. Chuvaev, A. A. Filatenkov, T. Glodariu, A. Koning, A. J. M. Plompen, S. M. Qaim, D. L. Smith, and H. Weigmann, Phys. Rev. C, 71 (2005) 044617.

[35] Kong Xlangzhong, et al., Rept.: Chinese report to I.N.D.C. No. 042 (1997) 9.

[36] Y. Kasugai, et al., Conf.: JAERI-M Report No. 92, 27 (1992) 268.

[37] Y. Ikeda, et al., Conference: JAERI-M Report No. 92, 27 (1992) 268.

[38] S. C. Gujarathi and S. K. Mukherjee, Indian J. Phys. 41 (1967) 667.